Structural Determination of β-SiC(100)-$c(2 \times 2)$ from C-1s Surface-Core-Exciton and Si-2p Absorption

J. P. Long,[1] V. M. Bermudez,[1] and D. E. Ramaker[1,2]
[1]*Naval Research Laboratory, Washington, DC 20375*
[2]*Chemistry Department, George Washington University, Washington, DC 20052*
(Received 7 June 1995)

The marked polarization dependences of two C-1s surface-core-exciton transitions—as revealed by near-edge x-ray absorption fine structure on single-domain β-SiC(100)-$c(2 \times 2)$—are used, together with Si-2p absorption and molecular orbital cluster calculations, to settle the long-standing controversy over the structure of this surface. The surface is terminated with staggered rows of unusual, nearly triply-bonded C dimers bridging underlayer Si dimers. Resonant valence-band photoemission accompanying C-1s exciton autoionization reveals directly the electronic structure of the C dimers.

PACS numbers: 78.70.Dm, 73.20.At, 79.60.Bm

The pronounced near-edge x-ray absorption fine structure (NEXAFS) observed at many core edges often reflects variations in the local unoccupied density of states (DOS) near the core. Probing the *surface* DOS becomes possible by detecting NEXAFS via the electrons, or their secondaries, that are ejected with short escape depths when the core hole decays via Auger or autoionization channels. Surface sensitivity allows the orientation of unoccupied p orbitals of surface atoms to be found, in principle, from the characteristic $\cos^2(\phi)$ dependence of the dipole absorption from a 1s core level, where ϕ is the angle between the p-orbital axis and the x-ray electric field $\vec{E}$. This approach has been used to determine the orientation of many simple molecules *adsorbed* on ordered surfaces [1] and even of bonds to *adsorbed* atoms [2]. Until now, however, the structures of *intrinsic* surfaces have not been similarly explored.

The problem with intrinsic surfaces occurs largely because bulk- and surface-adsorption features of the same element overlap. This problem may be alleviated in the case of surface-core excitons (SCE), which are distinguished from the bulk background by narrow line shapes or by transition energies falling below the bulk onset. Previous NEXAFS studies have thus identified SCE's on several intrinsic surfaces [e.g., cation SCE's on III-V semiconductor (110) surfaces] but have not determined surface structures. In the case of III-V SCE's, only the ϕ dependence of autoionization emission (often called resonant photoemission), not of total absorption, has been reported but has not been usefully related to structure because it is affected by mixing between resonant and direct photoemission [3]. On diamond (111) 2×1, C-1s SCE's have also been observed [4], but neither a ϕ dependence of total absorption nor resonant photoemission has been demonstrated. C-1s excitons in both the σ^* and π^* systems of graphite have recently been verified [5], but a distinction between bulk and surface behavior has not been reported and is unlikely in this van der Waals–bonded solid.

β-SiC is a cubic, wide band gap (2.38 eV) semiconductor having promise in high temperature and blue-emitting optoelectronic devices. The C-terminated (100) surface, which reconstructs as $c(2 \times 2)$, is important for its chemi-

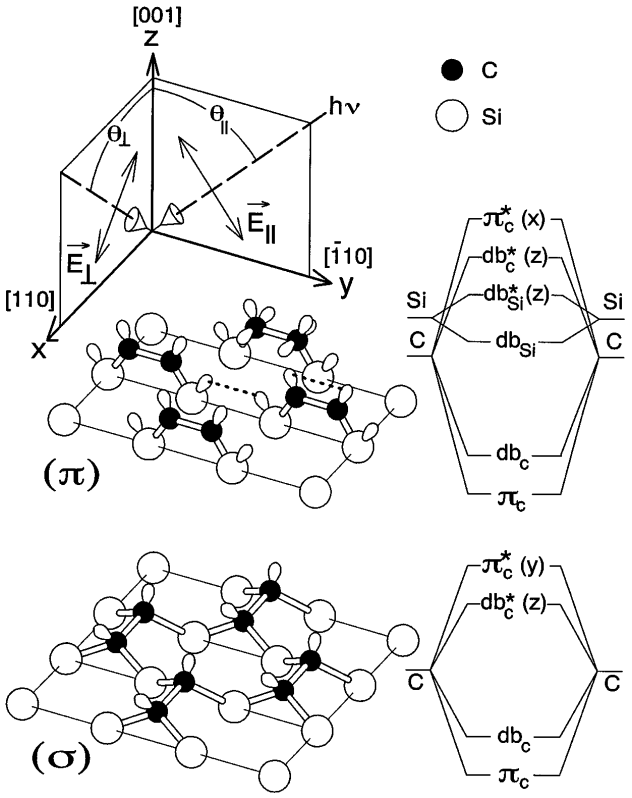

FIG. 1. Definitions of polarization and angle of incidence for the two previously proposed $c(2 \times 2)$ surface topologies, π and σ. Only the terminating C layer and the Si underlayer are sketched. Dangling atomic-basis orbitals are indicated; dotted lines show dimer interactions. For clarity in the π model, the p_x orbitals are shown only for one C dimer. Energy level diagrams show schematically the results of MO cluster calculations. Predominant orientations of p-related DOS for empty dangling bond (DB*) and π^* MO's are given in parentheses.

0031-9007/96/76(6)/991(4)$06.00

cal inertness and thermal stability [6]. Two structures, the π and σ models sketched in Fig. 1, have been proposed and have remained controversial both experimentally [7,8] and theoretically [9–12] for years. Here we establish conclusively that the π structure is correct through the separate polarization dependence of two, intense C-1*s* SCE resonances. This conclusion is further supported both by Si $L_{2,3}$-edge NEXAFS, which provides evidence for a Si dangling bond state that is present only in the π model, and by molecular orbital (MO) cluster calculations, which reveal the presence of this Si state and which predict the polarization dependences of the C-1*s* resonances. This work thus verifies a recent *ab initio* calculation [12] and an earlier semiempirical one [9] that found the π structure to be energetically favored. Both calculations found for the C-C dimers and unusual triple-bond character, without precedent in surface reconstructions, which occurs through an interaction between the two dangling bonds (DB's) as indicated by a dotted line in Fig. 1. Our polarization results are the first to verify this picture. In addition, we find that the electronic structure of these surface C dimers is revealed through the strong resonant photoemission of their valence states that accompanies the autoionizing deexcitation of the C-1*s* SCE. This first demonstration of surface resonant photoemission at the C *K* edge contrasts with other C *K*-edge resonant photoemission studies, e.g., on graphite [5] or C_{60} [13], which have given data characteristic of the bulk.

Angle-integrated electron spectra were obtained with a double-pass cylindrical mirror analyzer (CMA) on beam line X24C at the National Synchrotron Light Source (NSLS). β-SiC films (*n*-type, $N_d \approx 10^{17}\,\mathrm{cm}^{-3}$, $\sim$5 μm thick), grown *ex situ* by chemical vapor deposition on Si(100) wafers [14], were prepared in ultrahigh vacuum ($<3 \times 10^{-10}$ torr) as noted elsewhere [6,7,15]. The wafers were cut 0.5° from [001] toward [110] to elicit single domain reconstructions. Figure 1 defines our polarizations $E_\perp$ and $E_\parallel$ and angles of incidence θ relative to the previously proposed π [8] and σ [7] structures. The direction of the Si bonds was found with low-energy electron diffraction (LEED) from the orientation of the Si-terminated, single-domain, (2×1) reconstruction [15,16] upon which H-free $c(2 \times 2)$ was subsequently formed by decomposition of ethylene at 1100 °C [7,8]. The alternative preparation of $c(2 \times 2)$ by thermal desorption of Si from the Si-terminated (2×1) was rejected because of the likelihood for graphite contamination [7,8].

Figure 2 shows C-1*s* NEXAFS data obtained by constant final state spectroscopy (CFS), where the yield vs $h\nu$ of secondary electrons at fixed kinetic energy E_k is measured. The small escape depth of electrons with $E_k = 25$ eV (breadth 0.3 eV) enhances surface sensitivity. For the bulk-sensitive scan ($E_k = 4$ eV: larger escape depth), the marked decrease of the narrow resonance relative to the bulk absorption at larger $h\nu$ identifies it as surface derived [17]. This was confirmed by the near elimination of the resonance (not shown) after dosing with

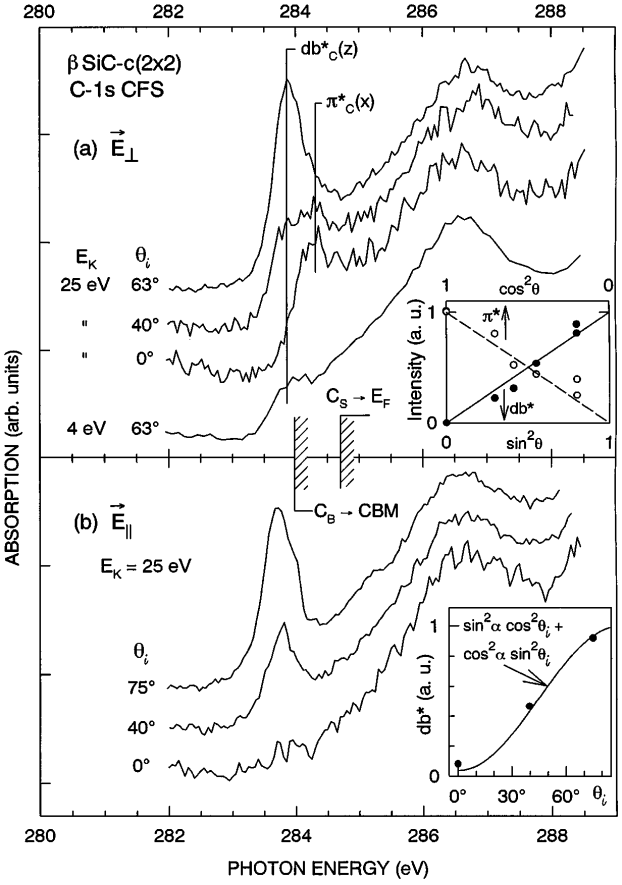

FIG. 2. Dependence of C-1*s* NEXAFS on θ_i and polarization (defined in Fig. 1). The partial yield (CFS) spectra are normalized for equal amplitudes in the bulk-absorption region around 287 eV and are offset vertically for clarity. Thresholds are marked for absorption from bulk (*B*) C to the conduction band minimum (CBM) and from surface (*S*) C to the Fermi level. Insets show angular dependences obtained from line fitting and predicted theory (see text). (a) $\vec{E}_\perp$: θ_i behavior for the two SCE's involving the two empty surface states comprising DB_C^* and π_C^* MO's. The weak bulk-sensitive response for $E_k = 4$ eV confirms surface character. (b) $\vec{E}_\parallel$: Single DB_C^* resonance in surface-sensitive mode.

atomic H. The hatched absorption thresholds in Fig. 2 are located from C-1*s* photoelectron spectra: The binding energy of the surface carbon C_S is 282.7 eV [relative to the valence band (VB) maximum], 1.1 eV larger than the bulk C_B. The resonances near 284 eV lie in the bulk band gap *below* the Fermi level and are therefore SCE's.

We now consider the polarization dependence and origin of the absorption resonances. Figure 1 illustrates qualitatively the energy levels of the frontier orbitals predicted from MO cluster calculations (AMPAC-AM1 [18]) for both π and σ models. We emphasize the polarization predictions, for which a MO approach is well suited. The C-1*s* polarization dependence was estimated by projecting out the p_x, p_y, p_z strengths on the surface C atoms for each antibonding MO. The dominant strength is given in parentheses in Fig. 1. In all cases, including cluster size dependence, the dipole transition strength when $\vec{E}$ is along

this axis exceeds 80% relative to the other axes. To include effects of the core hole, calculations were also performed with one surface C in the cluster replaced by N (the $Z + 1$, equivalent-core approximation) with the extra N electron removed so that the empty levels could be interpreted as a single-particle DOS.

In Fig. 2(a), the two C-1s SCE's at 283.9 and 284.4 eV exhibit intensities consistent with a $\sin^2(\theta_\perp)$ and $\cos^2(\theta_\perp)$ dependence (see inset), as predicted by the MO calculations with the assumption of dipole transitions. The points in the inset, which include additional data taken at slightly lower resolution, were determined from fitting sums of Gaussians with an error function onset [1]. The polarizations given in the energy level diagrams in Fig. 1 constrain the $\pi^*_C(x)$ state of the π model to be the $\cos^2(\theta_\perp)$ resonance. This resonance rules out the σ model, which has no empty states near the edge with predominant p_x character. In both models there is a state DB^*_C with predominant p_z character. This state originates from half-filled dangling atomic orbitals which form bonding (DB_C) and antibonding (DB^*_C) MO's through a dimer interaction (dotted line in Fig. 1). The $\sin^2(\theta_\perp)$ resonance for $E_\perp$ is attributed to this state, which is predicted to lie below the π^* state in the π model, as observed. This DB^*_C resonance is isolated (π^* is absent) for the azimuthal orientation of $E_\parallel$ [Fig. 2(b)]. The polarization dependence for this case is compared in the inset to the prediction of the equivalent-core MO calculation, which finds a value of 12° for α (the tilt angle of the dangling atomic orbital away from the normal); the noise level of the data at $\theta_\parallel = 0$ allows us only to constrain $\alpha < 16°$. The weakness of the transition measured for $\theta_\parallel = 0$ is a consequence of the significant DB_C-DB_C interaction within the dimer, which decreases α. If sp^2 hybridization prevailed, without dangling bond interaction, α would be 30°. The interaction splits DB_C and DB^*_C and lends triple-bond character to the C dimer. The observed small value of α thus confirms the unusual triple-bond character emphasized in more rigorous calculations [9,12].

The π structure is further verified by Si-2p NEXAFS (Fig. 3), which provides evidence for Si dangling bonds absent in the σ model. Two features, S_1 and S_2, appear in the difference spectrum [Fig. 3, curve 4]. Both S_1 (101–103 eV) and S_2 (105–107 eV) are identified as surface states by their E_k (i.e., escape depth) dependence. The Si-2p spin-orbit splitting of 0.61 eV contributes to the widths. S_1 is removed by H and is therefore ascribed to the DB^*_{Si} state formed from Si dangling orbitals by the Si-dimer interaction responsible for the calculated DB^*_{Si}-DB_{Si} splitting. This dimerization was previously proposed based on LEED [8] and has also been predicted in *ab initio* calculations [12]. Our assignment of S_1 is further supported by the similarity of our spectra to those of Shek *et al.* [19], who reported Si-2p CFS measurements from the Si-*terminated* β-SiC(100) surface, which possesses Si dangling bonds. Because S_2 is relatively unaffected by H, it is assigned to the antibonding companion of the backbond from a surface C to an underlying Si. While the MO cluster calculations locate both these states within the measured energy range, we note that multiple scattering [20] could contribute to the S_2 feature.

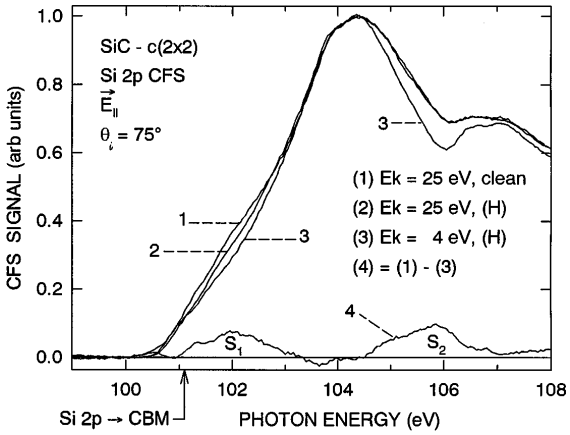

FIG. 3. Si-2p NEXAFS using bulk- ($E_k = 4$ eV) and surface- ($E_k = 25$ eV) sensitive modes for clean and hydrogenated surfaces. Curves are normalized at 104.4 eV. The single-particle absorption threshold inferred from Si-2p core-level photoemission is marked. The difference spectrum (curve 4) reveals empty states S_1 and S_2 assigned in the text.

The strong C-1s SCE resonance which facilitate the present work are a result of acetylenelike C dimers stabilizing the $c(2 \times 2)$ reconstruction. The dimers' relative isolation occasions narrow surface states with large effective mass that favor localization of the excited electron. The strength of the resulting transitions contrasts, for example, the weak SCE's reported for diamond (111)-2 × 1 and attributed to the extended surfaces states of this π-bonded chain reconstruction [4].

The strong localization of the SCE engendered by the isolated dimers also provides access to their electronic structure through resonant photoemission. Here one records the spectrum of valence electrons that are promoted when the SCE autoionizes, i.e., when the excited electron, by virtue of its localization, participates in deexcitation of the SCE by recombining with the core hole, leaving a one-hole (1h) state. This process is responsible for the strong resonant enhancement of VB photoemission in Fig. 4, as is evident after considering the competing contribution of on-resonance Auger decay, where the excited electron remains as a spectator, leaving a two-hole, one-electron (2h1e) state. (Ordinary 2h Auger decay becomes important for larger $h\nu$ values when the excited electron vacates the core hole.) In Fig. 4, the dashed curve gives a rough estimate of the 2h1e contribution, obtained by an iterative procedure involving the self-fold of the on-resonance VB. It is clear that the on-resonance VB emission occurs predominantly through 1h autoionization. That the resonant VB emission stems from the SCE was verified with constant initial state (CIS) spectra (inset to Fig. 4), which depended on polarization and H dosing

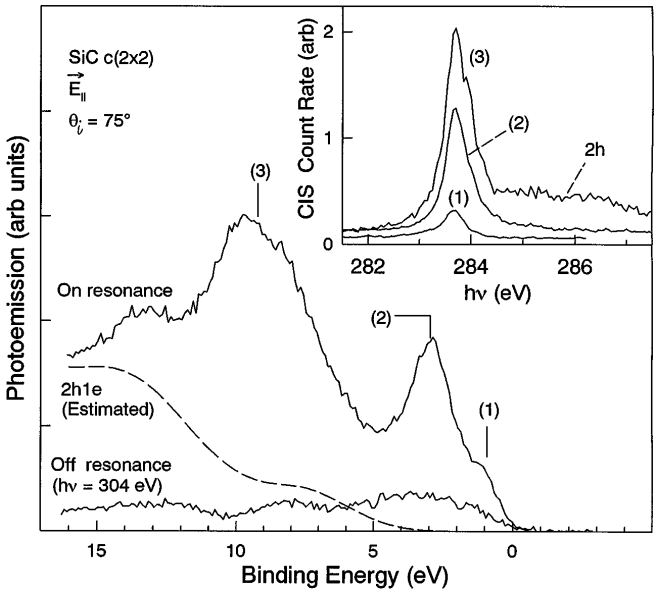

FIG. 4. VB spectra for $h\nu$ both on and off the DB_C^* resonance. Dashed curve is explained in the text. Inset: CIS spectra for initial-state energies as marked in the VB. Amplitudes are as measured (no relative scaling).

identically to CFS spectra. In CIS spectra, the $h\nu$ dependence of emission from a preselected initial state is recorded by scanning the CMA along with $h\nu$. The CIS emission tail at larger $h\nu$ for state (3) is 2h Auger emission from surface, bulk, or both.

The on-resonance VB exhibits new surface-C features absent from spectra taken off resonance, e.g., at $h\nu = 304$ eV in Fig. 4 and at other $h\nu$ values down to 45 eV. This is in contrast to the bulklike resonant VB spectra reported for graphite [5] and C_{60} [13]. The dominance of the surface emission means that the occupied DOS localized on the surface carbons is revealed directly, albeit modulated by the autoionization matrix element. No calculations are available for comparison, although a distinct surface electronic structure has been predicted for both an ideally terminated and a hypothetical (2×1), C-terminated surface [21]. The data in Fig. 4 may permit an unusually clear testing of layer-, atom-, and angular-momentum-resolved DOS calculations and should improve understanding of core-hole perturbations, a more likely prospect now that the surface topology has been firmly established.

We wish to acknowledge helpful discussions with M. N. Kabler, R. Kaplan, J. C. Rife, and M. L. Shek and thank L. Matus and colleagues at the NASA-Lewis Research Center, Cleveland, OH, for providing the β-SiC samples. Part of this work was done at NSLS, which is supported by Department of Energy Contract No. DE-AC02-76CH00016. Support by the Office of Naval Research is also gratefully acknowledged.

[1] J. Stöhr, *NEXAFS Spectroscopy*, edited by R. Gomer, Springer Series in Surface Sciences Vol. 25 (Springer-Verlag, Berlin, 1992).
[2] D. Purdie *et al.*, Phys. Rev. B **48**, 2275 (1993).
[3] C. Janowitz *et al.*, Surf. Sci. **275**, L669 (1992).
[4] J. F. Morar *et al.*, Phys. Rev. B **33**, 1346 (1986).
[5] P. A. Brühwiler *et al.*, Phys. Rev. Lett. **74**, 614 (1995).
[6] R. Kaplan and V. M. Bermudez, in *Properties of Silicon Carbide—EMIS Data Reviews Series No. 13*, edited by G. L. Harris (INSPEC, London, 1995), p. 101.
[7] V. M. Bermudez and R. Kaplan, Phys. Rev. B **44**, 11 149 (1991).
[8] J. M. Powers *et al.*, Phys. Rev. B **44**, 11 159 (1991).
[9] P. Badziag, Phys. Rev. B **44**, 11 143 (1991).
[10] B. I. Craig and P. V. Smith, Surf. Sci. **256**, L609 (1991).
[11] H. Yan, X. Hu, and H. Jónsson, Surf. Sci. **316**, 181 (1994).
[12] H. Yan, A. P. Smith, and H. Jónsson, Surf. Sci. **330**, 265 (1995).
[13] P. A. Brühwiler *et al.*, Chem. Phys. Lett. **193**, 311 (1992).
[14] J. A. Powell, L. G. Matus, and M. A. Kuczmarski, J. Electrochem. Soc. **134**, 1558 (1987).
[15] R. Kaplan, Surf. Sci. **215**, 111 (1989).
[16] S. Hara *et al.*, Phys. Rev. B **50**, 4548 (1994).
[17] The requisite variation of escape depth with E_k was confirmed with Si-2p PES: V. M. Bermudez and J. P. Long, Appl. Phys. Lett. **66**, 475 (1995).
[18] M. J. S. Dewar *et al.*, J. Am. Chem. Soc. **107**, 3902 (1985).
[19] M. L. Shek *et al.*, J. Vac. Sci. Technol. A **12**, 1079 (1994).
[20] J. J. Rehr, R. C. Albers, and S. I. Sabinsky, Phys. Rev. Lett. **69**, 3397 (1992).
[21] L. Wenchang, Y. Weidong, and Z. Kaiming, J. Phys. Condens. Matter **3**, 9079 (1991).